Biophysics, Vol. 50, No. 6, 2005, pp. 65–70. Translated from Biofizika, Vol. 50, No. 6, 2005, pp. @@–@@.

CELL BIOPHYSICS

Dynamic Heterogeneity of Phospholipid Bilayer and Diffusion of Molecules at the Interface

Ye. V. Tourleigh[a], K. V. Shaitan[a], and N. K. Balabaev[b]

[a] *Moscow State University, Vorob'evy gory, Moscow, 119992 Russia*
[b] *Institute of Mathematical Problems of Biology, Russian Academy of Sciences, Pushchino, Moscow Region, 142290 Russia*

Received March 11, 2005

Abstract—The method of steered molecular dynamics was developed to evaluate the kinetic parameters of penetration of molecules through the interface. Heterogeneous microviscosity of a membrane was calculated for a hydrated 1-pamitoyl-2-oleyl-*sn*-glycero-3-phosphatidylcholine bilayer. Effects of the chemical properties of penetrant molecule on its translocation through the membrane were studied.

Key words: molecular dynamics, membranes, diffusion

INTRODUCTION

The molecular dynamics (MD) of heterogeneous and membrane structures is currently of great interest and is used in fundamental studies of the dynamic behavior of such systems. Detailed experimental investigation of local physical and chemical properties and dynamics of biological membranes is also of considerable interest but attended with certain difficulties [1, 2]. This is especially true for microscopic considerations of mass- and energy transfer in very anisotropic structured heterogeneous media and for the building and equilibration of nonequilibrium supramolecular structures. In this paper, the MD method employing an all-atom force field, special procedures, and relatively long trajectories, was used for specification of the macroscopic picture of diffusion processes at the interface between aqueous and membrane phases [3–5]. The investigated membrane system has a high degree of hydration, which allowed minimization of the effects of periodic boundary conditions. To maintain constant temperature conditions, we used a collisional thermostat [6–8], which does not lead to nonlinear attractor regimes distorting statistical equilibrium in energy distribution by degrees of freedom [9, 10].

To estimate the microviscosity of the studied membranes in various parts of the anisotropic bilayer, as well as to study the how the structure of penetrants affect their interactions with membrane, a modified variant of steered molecular dynamics (SMD) was developed [11, 12]. SMD makes it possible to quantitatively estimate parameters, which characterizes the physical mechanisms of elementary actions of mass transfer in microheterogeneous structures [13].

EXPERIMENTAL

The molecular dynamics was calculated with the PUMA software package (developed and supported by IMPB RAS), which was specially modified to include SMD. The system of classical equations for atom movement was solved in the Amber99 force field [14].

The membrane bilayer was composed of 1-pamitoyl-2-oleyl-*sn*-glycero-3-phosphatidylcholine (POPG), which contained 64 lipid molecules (Fig. 1). In the initial structure, the direction of the longest molecular dimension was perpendicular to the membrane plane. The initial surface density of lipids was 66 Å^2, which was close to the experimental value (62–68 Å^2, [15–18]).

The parameters of potentials for the double bond in oleic residue and partial charges in POPG (Fig. 1) were taken from [19–22]. We used the TIP3P water model; the valence bonds and valence angles in water molecules were not fixed, but were instead determined by the corresponding potentials. In the initial configuration, water molecules were placed at a distance not less than 2.3 Å from the outermost atoms of membranes. The degree of solvation was 44 water molecules per one lipid molecule (full hydration of POPG requires at least 27 water molecules per lipid [23]).

The cutoff for van der Waals and Coulomb interactions was 16 Å. The smoothing procedure for van der Waals interactions involved multiplication of the Lennard-Jones potentials by the smoothing (switching) function $W(r)$:

$$W(r) = \begin{cases} 1, & r \le R_{on} \\ \dfrac{(R_{off}^2 - r^2)^2 (R_{off}^2 - 3R_{on}^2 + 2r^2)}{(R_{off}^2 - R_{on}^2)^3}, & R_{on} < r < R_{off}, \\ 0, & r \ge R_{off} \end{cases}$$

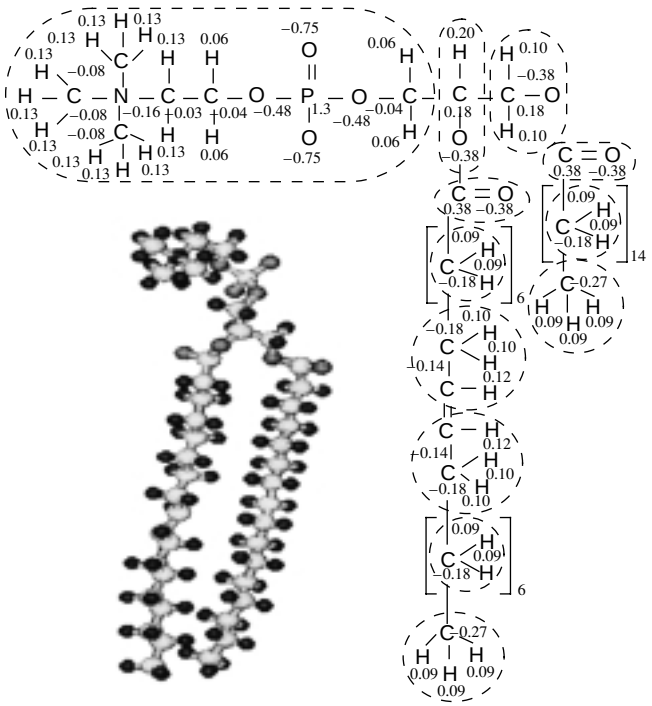

Fig. 1. Charge distribution in a lipid molecule. Electroneutral groups are marked with a dashed line.

where r is the distance between the interacting atoms, R_{on} parameter was 15 Å, and R_{off} was 16 Å. The Coulomb potential was scaled by the screening function:

$$W(r) = \begin{cases} (1 - r/R_{off})^2, & r \le R_{off} \\ 0, & r > R_{off}. \end{cases}$$

The dielectric constant was assumed to be unity. The step of numeric integration was 1 fs.

Periodic boundary conditions were imposed on the system. The calculations were performed both under the conditions of a constant bilayer area and pressure towards the membrane normal (NP_z-*AT* ensemble) and under constant pressure in all three directions (*NTP* ensemble). Constant-pressure condition was achieved by using the Berendsen barostat [24] with equal frequencies in three directions, which varied from 0.1 to 1 ps^{-1}. To consider the effects of the bilayer surface tension, the lateral component of barostatic pressure was assumed to be negative [25]. (It should be kept in mind that, according to the Pascal law, the pressure in the aqueous phase of a system is equal in all directions. Consequently, the real tension pressure in the membrane is somewhat higher than the pressure applied to the water–membrane system.) A virtual collision medium was used for a maintaining constant temperature of 300K [7]. The mean frequency of collisions with virtual particles was 10 ps^{-1}, and the weight of virtual particles was 1 amu.

RESULTS AND DISCUSSION

The POPG bilayer was subjected to multistep equilibration. Preliminary equilibration of the bilayer was performed at T = 300 K and isotope barostating at 1 atm (barostatic frequency, 0.2 ps^{-1}). Then, membrane was deliberately stretched by linear increase in the lateral dimensions of simulation box. This technical approach allowed us to set the system into a state in which the area of the membrane corresponded to the experimental value. Then, the system was further equilibrated for 750 ps under NP_z–*AT*-conditions. Mean lateral pressure component at this part of the trajectory was –330 atm. The mean membrane normal component was –118 atm. Total equilibration time was 1 ns (then followed by the working region of the trajectory; in the other cases, the duration of equilibration is implicitly stated). At the working part of the trajectory, we performed barostating at a frequency of 1 ps^{-1} and a mean pressure of P_x = P_y = –260 atm in the XY plane (which is parallel to the membrane plane) and P_z = 1 atm in the normal direction.

After the equilibration, basic membrane characteristics such as surface tension, surface density of lipids, radial distribution functions of atoms in the bilayer plane, the width of bilayer, distribution of atomic groups along the membrane normal, and parameters of order for lipid chains agree in general with the data obtained in other computer investigations and experimental data [3, 15–18, 26–34].

Heterogeneity of the membrane system affects its interactions with penetrant molecules. For computation of the parameters which determine diffusion of molecules in the membrane, we used the SMD method [11, 12]. External forces (constant and alternating) were applied to some parts of the system. We used testing spheres of 18 Da with radii of 2 and 4 Å (i.e., an order of the radius of the carbon atom and a small functional group, respectively), which interact with the other atoms only by van der Waals forces (interaction constant ε, 0.15 kcal/mol). Constant external force F_{ext} was applied along the normal or in the membrane plane. In the first case, the testing sphere was preliminary fixed at 2 Å from the membrane; in the second case, it was placed in the center of the membrane, before the membrane was equilibrated for 2 ps. Then, we applied a force of 0.3 kcal/mol $Å^{-1}$ to 4 kcal/mol $Å^{-1}$ (1 kcal/mol $Å^{-1}$ = 7×10^{-6} din). In the case of the 2-Å sphere, the force value was 10 kcal/mol $Å^{-1}$ (Fig. 2).

According to the test simulations, a constant force of 10 kcal/mol $Å^{-1}$ drives the 2- and 4-Å spheres in the TIP3P water with mean rates of 10 and 2.6 Å/ps, respectively. The deviation from the hydrodynamic Stokes equation was had two causes. First, the particle radii exceeded the range of applicability of the homogeneous medium approximation. Second, the value of applied force and, consequently, the motion rate were relatively high, and the condition of laminar flow did not hold as well. However, the Stokes equation could

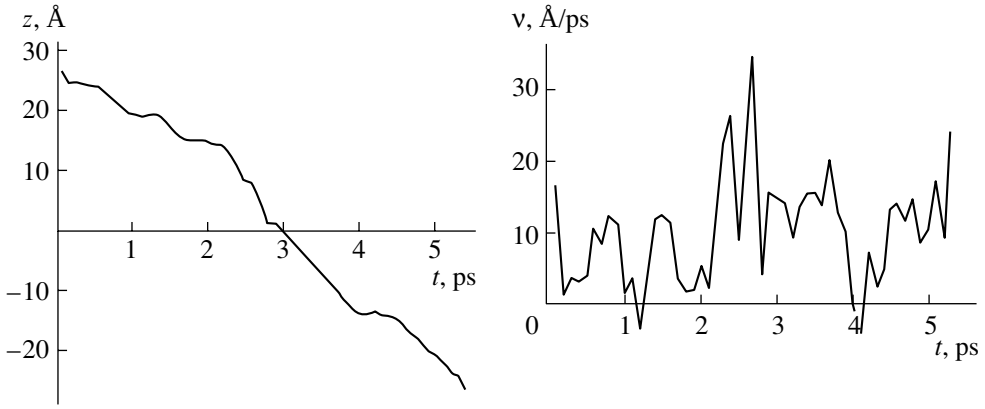

Fig. 2. Kinetics of movement of the testing van-der-Waals 2-Å sphere, subjected to a force of 10 kcal/mol Å^{-1} applied in the direction of the normal. (a) Position of the sphere on the *Z* axis (normal to the membrane). The center of the bilayer is located at $z = 0$; the borders, at $z = \pm 20$ Å. (b) The rate of sphere movement averaged over an interval of 0.1 ps.

also provide valid qualitative estimates at the microlevel [35]. Calculation of the SMD trajectories in the membrane system was stopped when the first van-der-Waals sphere permeated through the membrane, but for no longer than 2 ns. At forces of 1–10 kcal/mol Å^{-1}, the 2-Å spheres penetrated through the membrane in less than 2 ns. In the other cases, the spheres stacked up at the surface or penetrated into the membrane layer only to a certain depth. At forces below 1 kcal/mol Å^{-1}, the influence of medium perturbations on the 4-Å sphere was comparable to the effect of the applied force and, in some cases, the testing molecule also deviated from the initial position, away from the membrane, to distances up to 2 Å.

At the above-critical forces (for instance, 1 kcal/mol Å^{-1} for a 2-Å sphere), the molecules penetrated the membrane relatively rapidly. The penetration rate in this case is determined mainly by the external force, whereas the contribution by diffusion is relatively low.

The values of laterally applied forces F_{ext} were 1, 2, 4, and 10 kcal/mol Å^{-1}. For $F_{ext} = 1$ kcal/mol Å^{-1}, we analyzed the kinetic characteristics at the 75-ps part of the trajectory, when the particle remained at the center of the bilayer.

The coefficient of viscous friction γ was defined as the ratio of external force to the rate of particle drift:

$$\gamma = \frac{F_{ext}}{\nu}.$$

Formally, the friction coefficient could be redefined in terms of diffusion coefficient, using the known Einstein equation, and in terms of microviscosity of the media using the Stokes equation. It is noteworthy that in this case the Stokes equation is inapplicable. As to the Einstein equation, a special study is needed to verify its applicability in this particular situation, which is beyond the scope of this paper.

Currently, limited data are available on the viscosity when a particle moves along the normal to membrane surface or in the lateral direction in the middle of the bilayer. Experimental averaged viscosities of the surface layer range from 30 to 190 cP in various lipid membranes [36–38]. The experimental estimate of the mean viscosity of POPG is about 18 cP [39]. Since the microviscosities are not the same in different regions of the membrane, it is reasonable to define several structurally and dynamically inhomogeneous regions. In the first approximation, one can distinguish the regions of lipid heads and alkyl chains. Figure 3 shows the friction coefficients in terms of microviscosity for various

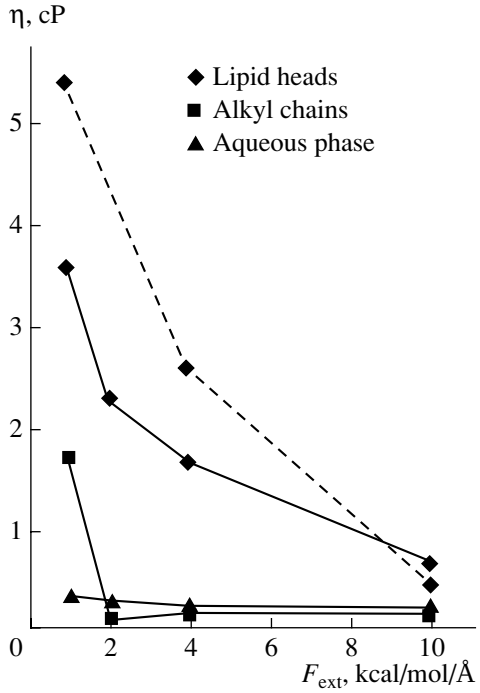

Fig. 3. Effective microviscosity in the POPG–water system. The radius of the testing van der Waals sphere is 2 Å. The solid line shows the system after preliminary equilibration for 500 ps; the dashed line, after complete equilibration for 1 ns.

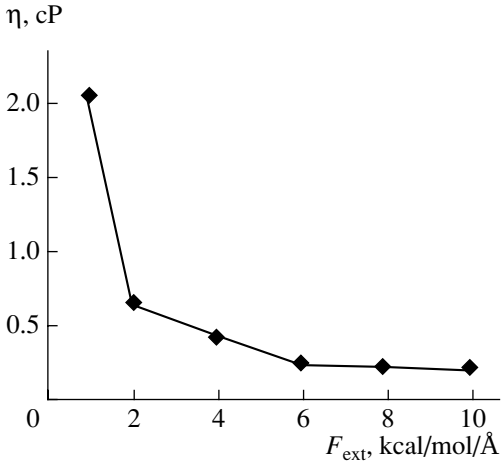

Fig. 4. Effective microviscosity in the center of the POPG bilayer. The radius of testing van-der-Waals sphere is 2 Å.

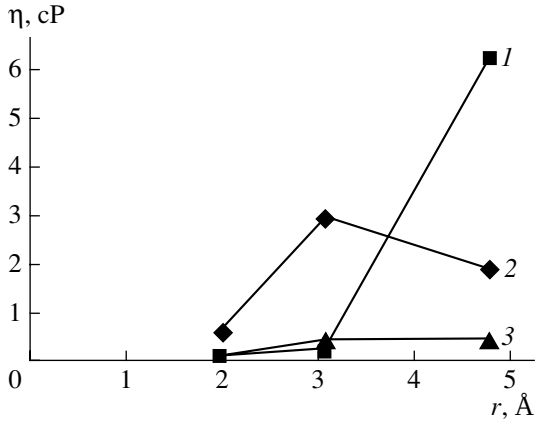

Fig. 5. Dependence of microviscosity on the effective radii of testing molecules in the POPG–water system. Total F_{ext} = 10 kcal/mol Å^{-1}. Notations: *1*, alkyl chains; *2*, lipid heads; *3*, aqueous phase.

regions of the system plotted against the external force applied to a 2-Å particle in the direction of the normal to the membrane plane.

Calculated values of effective viscosity of water for a 2-Å sphere are 0.3–0.4 cP, which is two to three times lower than the experimental values. These data agree with the known estimates of water viscosity for the TIP3P model [40]. Transverse viscosity of the membrane does not exceed 6 cP. Viscosity of the central part of the bilayer is several times lower than this value.

Data on the lateral movement of the sphere under influence of force are presented in Fig. 4. In this case, the effective microviscosity is very close to that measured in the region of alkyl tails in the direction of the normal.

It is noteworthy that for 2-Å particles, the Stokes equation in the region of alkyl tails is almost inapplicable. In general, the results suggest a non-Newtonian character of the medium and a weakly nonequilibrium state of this system at movement rates of 1–10 Å/ps.

The rate of penetration of the molecule under the influence of external force also depends on the chemical properties of the molecule. For comparison, we calculated the dynamics of penetration of tryptophan (effective radius, 4.8 Å) and alanine residues (effective radius, 3.1 Å), as well as of the 2-Å van-der-Waals sphere, into the bilayer. The obtained values of effective microviscosity are shown in Fig. 5. In the case of multiatom molecules, the force was applied uniformly to all the atoms of the system.

It should be noted that a more polar tryptophan residue has a higher rate in the region of lipid heads than the alanine residue, which, consequently, provides a lower value of microviscosity. In the region of hydrophobic alkyl chains, the situation is the reverse, with rates differing by a factor of 15. The region of lipid heads is most sensitive to the nature of a molecule moving through the membrane. Conversely, the hydrophobic core of the bilayer with a larger free volume is sensitive to the size of particles.

An example of forced transmembrane transport of alanine residue (Fig. 6) allows us to reveal the presence of factors facilitating recurring transmembrane movement related to the effects of structural memory in the bilayer. Pore formation, which accompanies molecule movement through the tetradecane monolayer, was studied earlier [41]. The effect of formation of a long-living pore in lipid membranes was not observed at the same values of external force. Both before and after the first translocation through the membrane, alanine residue spends a certain time in the adsorbed state and then rapidly (compared to the movement in the water phase) passes through the membrane.

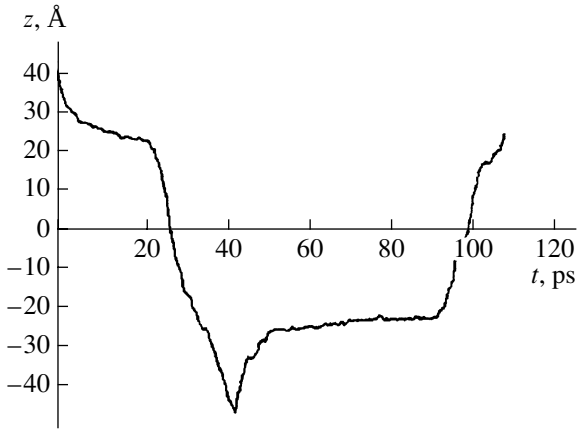

Fig. 6. Dynamics of movement of alanine residue through the lipid membrane. The position of the geometric center of the residue is shown. The borders of bilayer are located at ±22 Å. At the point of sharp bend of the curve, the direction of the force was inversed.

CONCLUSIONS

In this paper, we developed the method of "computer viscosimetry," which makes it possible to reveal the difference in diffusive properties of various molecules and to determine the effective viscosity characteristics in microheterogeneous structures, which are difficult to measure in conventional experiments. It should be noted that the terms viscosity and microviscosity in such systems require specific clarifications. In fact, we consider a quantitative characteristic of local dissipative properties expressed in units of viscosity. The hydrodynamic Stokes equation can only be used for estimating the order of magnitude of this characteristic. In this case, calibration of microviscosity in the defined range of forces is required for particles of particular size and chemical composition.

Anisotropic microviscosity in different regions of the bilayer can vary by an order of magnitude or even more. Considerable rates of molecule penetration into the bilayer in time scale of about 2 ns were found only when the value of external force is above a critical value. The critical force value increases with the radius of the molecule. Nonequilibrium effects appear at rates exceeding 1 Å/ps.

The greatest difference in effective microviscosity, depending on the chemical nature of the penetrant molecule, was found in the region of lipid heads.

The friction coefficients in the membrane normal direction, obtained for the above-critical forces value (approximately 1 kcal/mol/Å), do not exceed 6 cP in terms of effective microviscosity. The viscosity of the central region of the bilayer for the van-der-Waals sphere was found to be an order of magnitude lower than the surface region. At forces exceeding the critical value, there is a time delay in particle penetration into the membrane, the delay decreasing with an increase in the force. The viscosity of the central region of the bilayer in the lateral direction was close to the viscosity of the region of alkyl chains, when the force is applied in the direction of the normal.

ACKNOWLEDGMENTS

The work was supported by the Ministry of Education and Science of the Russian Federation (project no. I0431), the Integratsiya Foundation for Special Research Programs (project no. 01.106.11.0001), the Russian Foundation for Basic Research (project no. 04-04-49645), the Moscow government, and the company MKNT, Ltd.

REFERENCES

1. S. Tristram-Nagle, H. I. Petrache, and J. F. Nagle, Biophys. J. **75**, 917–925 (1998).
2. S. Tristrum-Nagle, Y. Liu, J. Legleiter, and J. F. Nagle, Biophys. J. **83**, 3324–3335 (2002).
3. H. Heller, M. Schaefer, and K. Schulten, J. Phys. Chem. **97**, 8343–8360 (1993).
4. K. V. Shaitan and P. P. Pustoshilov, Biofizika **44** (3), 436–441 (1999).
5. N. K. Balabaev, A. L. Rabinovich, P. O. Ripatti, and V. V. Kornilov, Zh. Fiz. Khim. **72** (4), 686–689 (1998) [Russ. J. Phys. Chem. **72** (4), 595–599 (1998)].
6. A. S. Lemak and N. K. Balabaev, Mol. Simul. **15**, 223–231 (1995).
7. A. S. Lemak and N. K. Balabaev, J. Comput. Chem. **17**, 1685–1695 (1996).
8. K. V. Shaitan and S. S. Saraikin, Zh. Fiz. Khim. **76** (6), 1091–1096 (2002) [Russ. J. Phys. Chem. **76** (6), 987–993 (2002)].
9. V. L. Golo and K. V. Shaitan, Biofizika **47** (4), 611–617 (2002).
10. V. L. Golo and K. V. Shaitan, Phys. Rev., Ser. E. (in press).
11. S. Park and K. Schulten, J. Chem. Phys. **120**, 5946–5961 (2004).
12. B. Isralewitz, M. Gao, and K. Schulten, Curr. Opin. Struct. Biol. **11**, 224–230 (2001).
13. K. V. Shaitan, Biofizika **39** (3), 949–967 (1994).
14. J. Wang and KollmanP. A. Cieplak, J. Comput. Chem. **21**, 1049–1074 (2000).
15. P. A. Hyslop, B. Morel, and R. D. Sauerheber, Biochemistry **29**, 1025–1038 (1990).
16. G. Pabst, M. Rappolt, H. Amenitsch, and P. Laggner, Phys. Rev., Ser. E **62**, 4000–4009 (2000).
17. J. M. Smaby, M. M. Mornsen, H. L. Brockman, and R. E. Brown, Biophys. J. **73**, 1492–1505 (1997).
18. R. W. Evans, M. A. Williams, and J. Tinoco, Biochem. J. **245**, 455–462 (1987).
19. T. R. Stouch, K. B. Ward, A. Altieri, and A. T. Hagler, J. Comput. Chem. **12**, 1033–1046 (1991).
20. S. E. Feller, D. Yin, R. W. Pastor, and A. D. Mackerell, Jr., Biophys. J. **73**, 2269–2279 (1997).
21. M. Schlenkrich and J. Brickmann, MacKerell A.D. Jr., Karplus M. *Biological Membranes: A Molecular Perspective from Computation and Experiment*, Ed. by K. M. Merz and B. Roux (Birkhauser, Boston, 1996), pp. 31–81.
22. A. L. Rabinovich, P. O. Ripatti, and N. K. Balabaev, J. Biol. Phys. **25**, 245–262 (1999).
23. K. Myrzyn, T. Rog, G. Jezierski, et al., Biophys. J. **81**, 170–183 (2001).
24. H. J. C. Berendsen, J. P. M. Postma, W. F. van Gunsteren, et al., J. Chem. Phys. **81**, 3684–3690 (1984).
25. S.-W. Chiu, M. Clark, V. Balaji, et al., Biophys. J. **69**, 1230–1245 (1995).
26. E. V. Turlei, K. V. Shaitan, and N. K. Balabaev, Biol. Membr. (in press).
27. R. Rand and V. Parsegian, Biochim. Biophys. Acta **998**, 351–376 (1989).
28. G. Pabst, Langmuir **16**, 8994–9001 (2000).
29. Z. Salamon, G. Lindblom, L. Rilfors, et al., Biophys. J. **78**, 1400–1412 (2000).
30. J. Seelig and A. Seelig, Q. Rev. Biophys. **13**, 19–61 (1980).

31. D. Huster, P. Muller, K. Arnold, and A. Herrmann, Biophys. J. **80**, 822–831 (2001).
32. M. Lafleur, P. R. Cullis, and M. Bloom, Eur. Biophys. J. **19**, 55–62 (1990).
33. M. J. Schneider and S. E. Feller, J. Phys. Chem. B **105**, 1331–1337 (2001).
34. R. A. Bockmann, A. Hac, T. Heimburg, and H. Grubmuller, Biophys. J. **85**, 1647–1655 (2003).
35. G. K. Batchelor, *Theoretical and Applied Mechanics. IUTAM Congress*, Ed. by W. T. Koiter (Elsevier, Amsterdam, 1976), pp. 33–55.
36. C. E. Kung and J. K. Reed, Biochemistry **25**, 6114–6121 (1986).
37. W. R. Dunham, R. H. Sands, S. B. Klein, et al., Spectrochim. Acta, Ser. A **52**, 1357–1368 (1996).
38. M. Sinensky, Proc. Natl. Acad. Sci. USA **71**, 522–525 (1974).
39. A. Sonnleitner, G. J. Schutz, and Th. Schmidt, Biophys. J. **77**, 2638–2642 (1999).
40. M. V. Mahoney and W. L. Jorgensen, J. Chem. Phys. **114**, 363–366 (2001).
41. E. V. Turlei, K. V. Shaitan, and N. K. Balabaev, Zhurn. Fiz. Khim. (in press).

SPELL OK